water

MDPI

Article

Impact Assessment of Pier Shape and Modifications on Scouring around Bridge Pier

Rashid Farooq [1,2,*] **and Abdul Razzaq Ghumman** [1,3]

1 Department of Civil Engineering, University of Engineering and Technology, Taxila 47080, Pakistan
2 Department of Civil Engineering, Faculty of Engineering and Technology, International Islamic University, Islamabad 44000, Pakistan
3 Department of Civil Engineering, College of Engineering, Qassim University, Buraydah 51431, Saudi Arabia
* Correspondence: rashidmeo50@gmail.com

Received: 10 July 2019; Accepted: 21 August 2019; Published: 23 August 2019

check for updates

Abstract: Previous experimental research on utilizing pier modifications as countermeasures against local scour has focused primarily on circular pier. It is of utmost importance to further investigate the most suitable pier shape for pier modification countermeasure separately and in combination. This experimental study aims to reduce the stagnation of the flow and vortex formation in front of the bridge pier by providing a collar, a hooked collar, a cable, and openings separately and in combination around a suitable pier shape. Therefore, six different pier shapes were utilized to find out the influence of pier shape on local scouring for a length–width ratio smaller than or equal to 3. A plain octagonal shape was shown as having more satisfactory results in reducing scour compared to other pier shapes. Furthermore, the efficiency of pier modification was then evaluated by testing different combinations of collar, hooked collar, cable, and openings within the octagonal bridge pier, which was compared to an unprotected octagonal pier without any modification. The results show that by applying such modifications, the scour depth reduced significantly. The best combination was found to be a hooked collar with cable and openings around an octagonal pier. It was revealed that the best combination reduced almost 53% of scour depth, as compared to an unprotected octagonal pier.

Keywords: scour; bridge pier; collar; cable; openings; hooked collar; countermeasures

1. Introduction

The mechanism of scouring process around bridge piers in rivers is of great importance to researchers in the field of hydraulic structures. The scouring process occurs because of the presence of a complex vortex system. This system consists of horseshoe vortex, wake vortex, trailing vortex, and bow wave vortex [1,2]. In recent years, several studies have been carried out to investigate the effect of different factors on the formation of vortex systems around bridge piers. These factors can be divided into three categories: (i) flow parameters, such as approach velocity and flow depth; (ii) sediment parameters, such as median size, size distribution, and sediment density; and (iii) pier shape, type, and dimension [3–8]. A key factor widely acknowledged as increasing the scour risk of bridges is pier shape. Pier shape plays a vital role in the formation and the strength of the vortex system [7,9–13]. The shape of the pier embedded vertically at the riverbed greatly changes the flow structures, and one can expect the large variations in the flow field due to different shapes of piers, and hence different scour forms.

Experimental and computational research have significantly enhanced the understanding of the local scour process around bridge piers by describing the underpinning science, particularly of the vortex systems and scour patterns around circular and rectangular pier shapes [2,14–20]. Recently, Manes and Brocchini [21] derived a new predictive formula to calculate the scour depth at piers, which merges the phenomenological theory of turbulence with empirical observations. On the contrary, studies on local scour process on cohesive sediment beds investigating efficient pier geometry from various pier shapes are rather inadequate (the most well-known being [7,13,22]). Nonetheless, a variety of suitable bridge pier shapes have been suggested by different researchers [23,24], based on limited experimental data. With the exception of a few aforementioned researchers, all others have chosen a circular shape for pier scouring study. Therefore, it is of utmost importance to consider different types of pier shapes and determine the most suitable pier geometry in terms of reducing scour. However, researchers are unanimous in that pier geometry alone is not sufficient to protect bridge piers against local scour [11,25–28].

Protecting measures in a pier against scouring will definitely decrease the likelihood of the bridge failure. The countermeasures against pier scour are broadly classified into two categories: bed-armoring countermeasures, and flow altering or pier modification countermeasures. The pier modification countermeasures include the provision of collars, cables, opening slots, hooked collars, etc. Collars of different shapes and varying thicknesses are practiced by many researchers around the bridge piers as protective plates against sediment removal [11,26,29–33]. According to Alabi [34], a collar that is thinner than 5 mm has no adverse effect on scour development. Zarrati et al. [4] found that the optimum width of a collar is thrice that of the pier, in terms controlling erosion. Thus, in the present study, the collar thickness of 5 mm and width of collar equal to three times that of the pier, was kept for all the experiments. EL-Ghorab [27] proposed openings countermeasure at the upstream side of a pier. These openings, starting from the upstream face of pier, continue transversely to lateral sides and straight to the downstream side. In his experiments, opening sizes equal to 10%, 15%, and 20% at vertical spacing of 0.5, 1.0, and 1.5 times the pier width, respectively, were utilized. He found that the opening size equal to 20% with vertical spacing 1.0 times the pier width was the best in decreasing flow pressure, thereby reducing the scour. Dey et al. [35] suggested threading or openings as an effective and easy-to-install countermeasure. Izadnia and Heidarpour [30] concluded that a cable–pier ratio of 0.15 was the most effective to countermeasure and weaken the downward flow effect. The provision of threading around a vertical pier is an economical technique used to minimize local scour. Saadati et al. [36] employed a hooked collar to investigate its effectiveness on maximum scour depth under clear water condition. Similarly, Chen et al. [37] evaluated the efficiency of hooked collars by examining different hooked collar placements within the bridge piers, which were compared to bridge piers without any collar. A hooked collar with a width of 1.25 b, a height of 0.25 b, and thickness of 5 mm, where b is the pier width, was used in his experiments. He concluded that the placement of a hooked collar at the bed level was efficient in reducing scour. Furthermore, the experiments conducted by the aforementioned researchers guided the placements of pier modification countermeasures, such as collars, cables, openings, and hooked collars, at piers for the present study.

However, a comprehensive review of pier modification countermeasures by Tafarojnoruz et al. [38] indicated a low efficiency in specific conditions or serious problems in practical applications. Tafarojnoruz et al. [39] noted that double-submerged vanes, bed sill, sacrificial piles, threading, collars, and pier slot can reduce the maximum scour depth by up to 35% in the best configurations. On the basis of these studies, a single pier modification countermeasure may not be adequate for pier scour reduction, whereas combined countermeasures may result in improvement.

The current literature on scour at bridge piers includes a large quantity of experimental work to understand the effect of pier shape on flow and scour. However, it has two key limitations when examined, particularly in the context of its usefulness for pier modifications. First, previous research has focused primarily on circular and rectangular piers, which are common in modern steel and concrete bridges that constitute the highway network in most countries. Only a few researchers with limited experimental data recommended the other pier geometries for scour reduction. Therefore, further experimental investigations are required by considering various pier shapes available in the literature to recommend the most suitable pier geometry in terms of reducing scour depth. Second, previous research has not captured adequately the response of different pier modifications on suitable pier geometry, individually and in combination. Zaratti et al. [11] and Farooq et al. [40], whose studies are the only few to consider the combined effect of modifications, used pier shapes other than circular. Other studies have typically assumed that a circular shape is suitable for pier modifications, for example Gaudio et al. [41], whereas, in practice, different pier modifications can be more effective by applying suitable pier shapes.

The aim of the present experimental study is to address directly the aforementioned two limitations and is thus novel in the following two aspects compared to previous experimental research. First, it characterizes the scour effects when different sediment sizes are used in combination with various pier shapes and modifications. Second, the most effective pier modification countermeasures available in the literature are considered, then individual and combined effect are examined on the most suitable pier geometry to experimentally derive the best combination. Lastly, previous studies have focused on the maximum scour depth and have given less attention to evaluating the extent of scour and volume of scour hole with pier modifications. This study is novel in its use of experimental data to derive a relationship between scour volume and maximum scour depth. This is of practical importance because bridge pier is known to increase the span-wise extent of scour in addition to increasing scour depth, and hence helpful to calculate the maximum volume of the material required for filling scour holes in post-flood remedial works.

2. Experimental Setup and Testing Procedure

2.1. Experimental Flume

All the experiments were performed in a smooth rectangular flume (20 m length, 1 m width, and 0.75 m depth) equipped with a recirculating water facility. The rectangular flume had a straight entrance, having a concrete base and side walls of 12 mm thick glass sheets. The flume was divided into three sections: inlet, working segment in the middle, and outlet. The flow was allowed to pass through the honeycomb placed at the inlet of the flume for obtaining smooth, fully-developed flow conditions at the working section. The working segment consisted of a 6 m long and 0.3 m thick layer of uniformly-graded fine sand material, in which the wooden pier was centered in the middle of the sand bed. At the end of the channel, there was a rectangular gated weir, which controlled and measured the discharge. For all experiments, the same flow conditions were maintained. Figure 1a,b shows a sketch of the experimental setup.

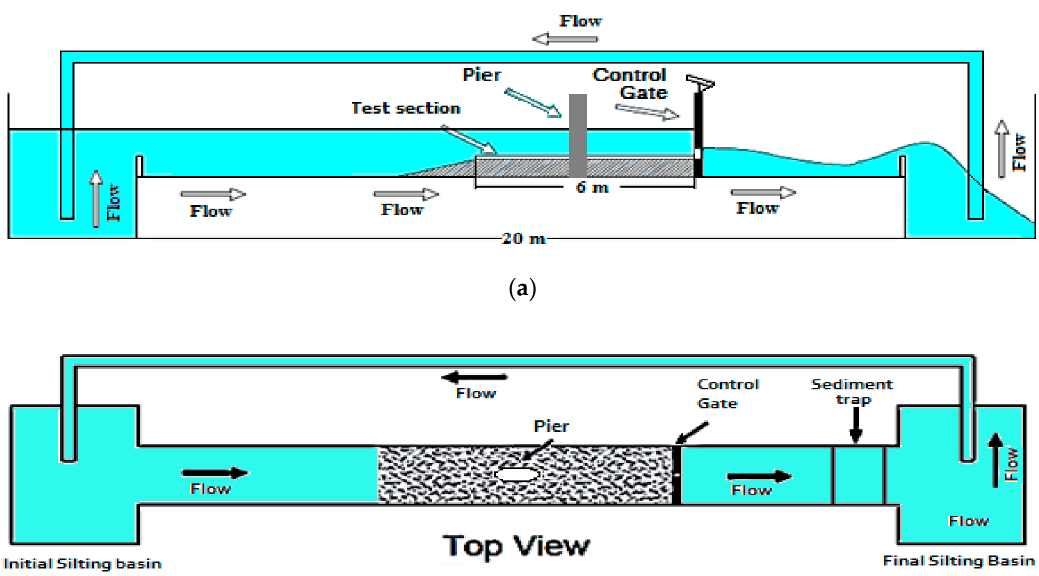

(a)

(b)

Figure 1. (**a**) Cross section of experimental rectangular flume, (**b**) Top view of experimental rectangular flume.

2.2. Sediment Bed

Two different median sediment sizes (d_{50} = 0.71 mm and 0.98 mm) were used for all the experiments. The geometric standard deviation of the particle size distribution, $\sigma_g = (d_{84}/d_{16})^{0.5}$, was 1.20 and 1.17 for the sediment sizes d_{50} = 0.71 mm and 0.98 mm, respectively (d_{84} and d_{16} being the sediment size for which the mass of the sediments were finer at 84% and 16%, respectively). The computed geometric standard deviation σ_g values of the two sediment beds were less than 1.3, which is the upper limit for uniformly graded sediment [42]. Similarly, the specific gravity and friction angles were S_g = 2.66, 2.67, and ϕ_s = 35°, 36.5°, for the sediment sizes d_{50} = 0.71 mm and 0.98 mm, respectively. Since D_p/d_{50} was more than 50 (D_p/d_{50} = 70.4 and 140.8), with D_p being the pier diameter, the effect of sediment size on the scour hole becomes negligible [43].

2.3. Flow Conditions

The flow discharge was selected in such a way that the normalized bed shear stress should not exceed the critical value for the incipient sediment movement at the plane sand bed of mean grain size (d_{50} = 0.71 mm and 0.98 mm). The experiments were conducted using a constant flow discharge of 0.075 m^3/s. The flow depths d_f in these experiments were 23 and 25 cm, corresponding to D_p = 5 cm and 10 cm, respectively, to neglect the flow shallowness effect, i.e., $d_f/D_p \geq 2.5$ [44]. The Froude number $\left(Fr = U/\sqrt{gh}\right)$ varied from 0.19 to 0.22, where U is the approach flow velocity, g is the gravitational constant, and h is the flow depth above the sediment bed. Table 1 presents the various flow parameters related to the experiments.

Table 1. Flow parameters for sand bed.

Discharge, (m^3/s)	Flow Depth, d_f (m)	Median Grain Size, d_{50} (m)	Approach Flow Velocity, U (m/s)	Critical Velocity, U_c (m/s)	Critical Shear Velocity, U_{*c} (m/s)	Flow Intensity, U/U_c	Critical Shields Parameter	Reynolds Number, Uh/v	Froude Number, F_r
0.075	0.23	0.00071	0.33	0.487	0.026	0.62	0.058	75462	0.22
0.075	0.25	0.00098	0.30	0.491	0.027	0.67	0.046	74568	0.19

The flow intensity was maintained approximately as U/U_c = 0.9 (clear water condition) in all the tests, where U is the approach flow velocity and U_c is the critical value for the inception of sediment motion. The critical shear velocity $U^*{}_c$ for sediments used in the current study was determined using the Shields diagram, as shown in Table 1. Critical velocity U_c in each experiment was calculated using the logarithmic average velocity equation for a rough bed as follows [45,46]:

$$\frac{U_C}{U_C^*} = 5.75\log\left(\frac{d_f}{k_e}\right) + 6, \tag{1}$$

where d_f is the flow depth and '$k_e = 2d_{50}$' is the equivalent roughness height.

2.4. Pier Geometry

Six different pier shapes, with each shape comprising two different diameters (D_p = 5 and 10 cm), were considered in the study, as shown in Table 2 where the associated values of D_p are summarized. Experiments were performed in the rectangular flume using the different pier shapes, such as circular (S_1), rectangular (S_2), rhombus (S_3), sharp nose (S_4), octagonal (S_5), and elliptical (S_6), to monitor the scour mechanism, with an aspect ratio of smaller than or equal to 3 (aspect ratio is pier length/width), under identical flow conditions. The ratio of channel width B to pier diameter, B/D_p, were 10 and 20 (see Table 3). The length of the pier L, except for the circular case, was kept at 15 cm for all different pier diameter shapes. Contraction scour seemed absent, since no bed degradation was observed over the contracted cross sections; this agreed well with Ballio et al. [47], who have suggested that contraction scour is negligible for $B/D_p \geq 10$. Hence, it is safe to state that contraction effects were not present in the current study.

Here, x, y, and z are the co-ordinates along transverse and bottom-normal to the flow, respectively. Origin (0, 0, 0) is taken at the center of the pier at the centerline of the flume over the bed surface. Geometric parameters of the six pier shapes (i.e., width, length, nose dimensions, etc.) are provided in Supplementary Table S1.

Table 2. Tested pier shapes and schematic diagram of measuring points of scour holes.

<table>
<tr><th>Pier shape</th><th>D_p (cm)</th><th>Scour Geometry</th></tr>
<tr><td>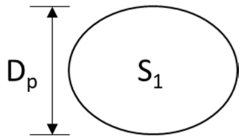</td><td rowspan="6">5; 10</td><td rowspan="6">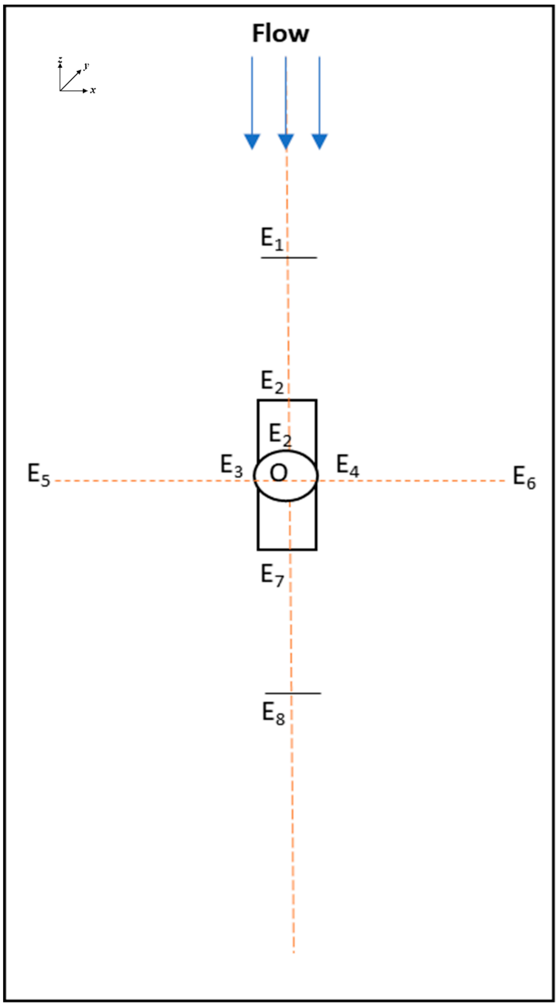

E_1—starting point of erosion at upstream
E_2—pier front at upstream
E_3 and E_4—edges of piers
E_5 and E_6—edges of scour hole along transverse direction
E_7—downstream end of pier
E_8—ending point of scour at downstream
O—origin
</td></tr>
<tr><td>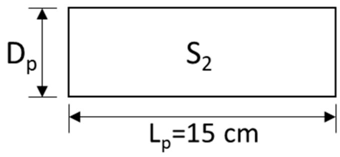</td></tr>
<tr><td>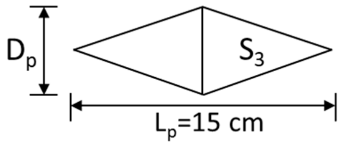</td></tr>
<tr><td>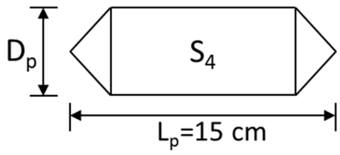</td></tr>
<tr><td>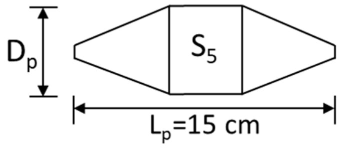</td></tr>
<tr><td>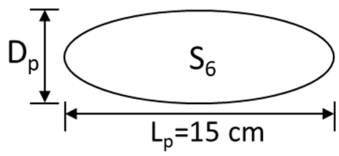</td></tr>
</table>

2.5. Pier Modification

Pier modification is very essential, as this component of bridge is directly affected by the scour action during normal and flood seasons. In the current study, the most effective pier modifications available in the literature, i.e., collar (C_o), cable (C_a), openings (O) and hooked collar (H), were utilized. The effect of pier modifications was analyzed separately and then in combination on the most suitable pier geometry. The possible combinations of pier modification around the most suitable pier geometry are openings with hooked collar (O-H), cable with hooked collar (C_a-H), openings with collar (O-C_o), cable with collar (C_a-C_o), openings with cable (O-C_a), openings with cable and hooked collar (O-C_a-H), and openings with cable and collar (O-C_a-C_o). A schematic of pier modifications around an octagonal pier is shown in Figure 2.

The following are the details of the pier configurations used in the current study:

- ➢ In all collar-pier experiments, the collar width was equal to thrice that of the pier, which was maintained.
- ➢ In all cable-pier experiments, a cable diameter to pier-width ratio of 0.15 was used. The vertical spacing between the cable loops was equal to the pier width, with each cable being parallel.
- ➢ In all openings-pier experiments, the diameter and vertical spacing of openings was 20% and 100% of the pier width, respectively.
- ➢ In all hooked collar experiments, a width of 1.25 D_p, a height of 0.25 D_p, and a thickness of 5 mm was placed at the bed around the bridge pier.

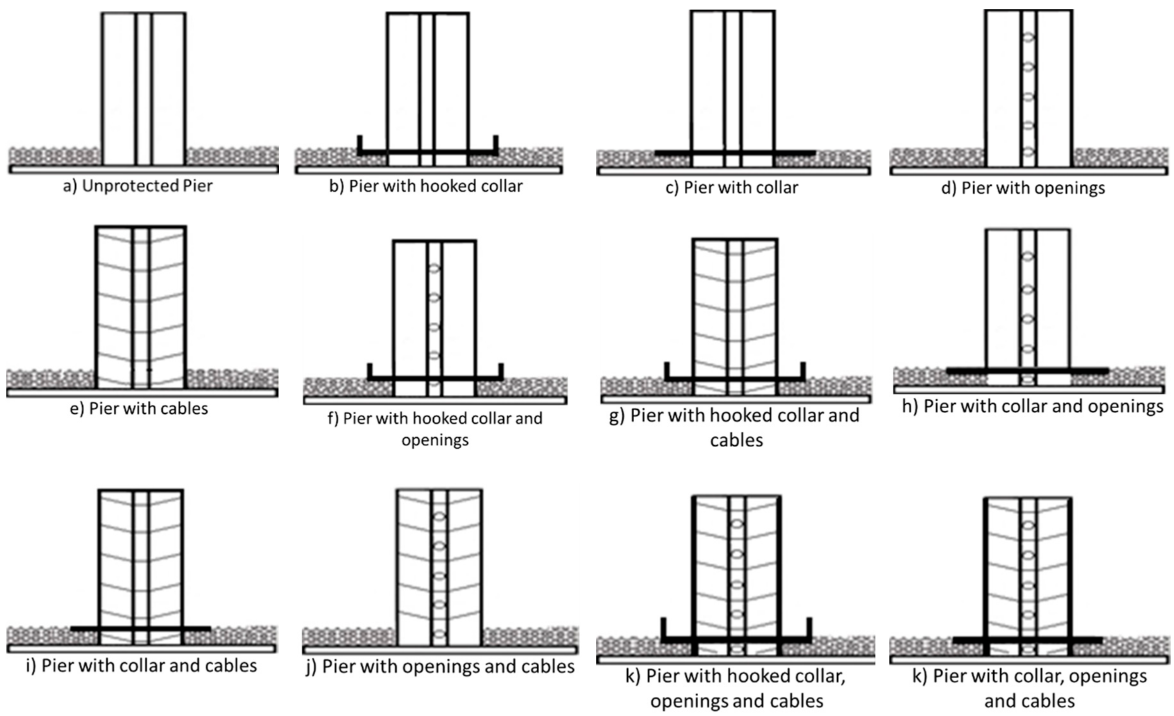

Figure 2. Details of pier modification around an octagonal pier.

2.6. Experimental Procedure

Experiments were performed in two phases. In the first phase, a series of 24 runs on six different pier shapes with different diameters (D_p = 5 and 10 cm) for two different median sediment sizes (d_{50} = 0.71 mm and 0.98 mm), all under a clear water scour condition, were performed. The values of the most important control variables and non-dimensional parameters characterizing the experiments, including those reported by Lança et al. [48], are summarized in Table 3.

Table 3. Characteristic control variables and non-dimensional parameters of experiments.

Test	Pier Shape	D_p (cm)	d_{50} (mm)	d_f (cm)	L/D_p	B/D_p	d_f/D_p	D_p/d_{50}	t_d (hrs)	d_{se} (cm)	d_{se}/D_p
1	S_1	5	0.71	23	-	20.0	4.6	70.4	24	12.9	2.57
2	S_1	10	0.71	25	-	10.0	2.5	140.8	24	15.8	1.58
3	S_2	5	0.71	23	3.00	20.0	4.6	70.4	24	15.6	3.12
4	S_2	10	0.71	25	1.50	10.0	2.5	140.8	24	19.7	1.97
5	S_3	5	0.71	23	3.00	20.0	4.6	70.4	24	12.1	2.42
6	S_3	10	0.71	25	1.50	10.0	2.5	140.8	24	15.2	1.52
7	S_4	5	0.71	23	3.00	20.0	4.6	70.4	24	13.9	2.78
8	S_4	10	0.71	25	1.50	10.0	2.5	140.8	24	18.3	1.83
9	S_5	5	0.71	23	3.00	20.0	4.6	70.4	24	10.3	2.07
10	S_5	10	0.71	25	1.50	10.0	2.5	140.8	24	11.8	1.18
11	S_6	5	0.71	23	3.00	20.0	4.6	70.4	24	13.3	2.65
12	S_6	10	0.71	25	1.50	10.0	2.5	140.8	24	16.3	1.63
13	S_1	5	0.98	23	-	20.0	4.6	51.0	24	13.1	2.62
14	S_1	10	0.98	25	-	10.0	2.5	102.0	24	16.2	1.62
15	S_2	5	0.98	23	3.00	20.0	4.6	51.0	24	15.7	3.14
16	S_2	10	0.98	25	1.50	10.0	2.5	102.0	24	19.8	1.98
17	S_3	5	0.98	23	3.00	20.0	4.6	51.0	24	12.5	2.50
18	S_3	10	0.98	25	1.50	10.0	2.5	102.0	24	15.4	1.54
19	S_4	5	0.98	23	3.00	20.0	4.6	51.0	24	14.2	2.84
20	S_4	10	0.98	25	1.50	10.0	2.5	102.0	24	18.6	1.86
21	S_5	5	0.98	23	3.00	20.0	4.6	51.0	24	10.7	2.14
22	S_5	10	0.98	25	1.50	10.0	2.5	102.0	24	12.1	1.21
23	S_6	5	0.98	23	3.00	20.0	4.6	51.0	24	13.5	2.70
24	S_6	10	0.98	25	1.50	10.0	2.5	102.0	24	16.4	1.64

Dp = pier diameter, d_{50} = median sediment size, d_f = flow depth, B = channel width, L = pier length, t_d = test duration, d_{se} = equilibrium scour depth.

In the second phase of experiments (similar to Khaple et al [49]), modifications were applied to the octagonal pier shape (S_5), as it reduces more scour depth when compared to other pier shapes. Hence, a series of 44 experiments were carried out by testing different pier modifications individually and in combination around two different pier diameters of octagonal piers (D_p = 5 cm and 10 cm), under clear water condition. In addition, two median sediment sizes (d_{50} = 0.71 mm and 0.98 mm) were used. The experimental data obtained from these tests are presented in Table 4. The experimental runs with median sediment size d_{50} = 0.71 mm were denoted by test X, which includes tests X_1–X_{22}; similarly, experiments with median sediment size d_{50} = 0.98 mm were denoted by test Y, which includes tests Y_1–Y_{22}.

The procedure of all experiments, performed in two phases, were similar. For instance, circular pier (S_1) was aligned vertically on the sand bed at a distance of 10.5 m from the upstream inlet end, wherein the sand bed was compacted and its surface was levelled with the adjacent concrete bed. The sand zone around the pier was covered with thin metallic plates to avoid uncontrolled scour at the beginning of the experiment. Then, the flumes were slowly filled with water to allow air entrapped in the sediment to escape. Once the flow depth and the discharge were established, the metallic plates were carefully removed, and the experiment started. The scour process was immediately initiated, and the scour hole depth at the upstream and sides of pier was measured every 12 min during the first hour (to the accuracy of ±0.1 mm), with the help of three point-gauges. Afterwards, the intervals between measurements increased. The outlet section was at the end of the test section, where the dislodged sand particles, if any, were deposited.

Table 4. Experimental data of modification around octagonal pier in uniform sediments. Hooked collar (*O-H*), cable with hooked collar (C_a-*H*), openings with collar (*O*-C_o), cable with collar (C_a-C_o), openings with cable (*O*-C_a), openings with cable and hooked collar (*O*-C_a-*H*), and openings with cable and collar (*O*-C_a-C_o).

Pier Shape	D_p	Modification	d_f (cm)	Series *X* d_{50} = 0.71 mm		Series *Y* d_{50} = 0.98 mm		Percentage Reduction of Scour Depth r_{ds} (%)	
				Test	d_s (cm)	Test	d_s (cm)	Test *X* d_{50} = 0.71 mm	Test *Y* d_{50} = 0.98 mm
S_5	5	*H*	23	X_1	8.1	Y_1	8.3	21.36	22.43
S_5	5	*Co*	23	X_2	8.5	Y_2	8.8	17.48	17.76
S_5	5	*O*	23	X_3	9.4	Y_3	9.9	8.74	7.48
S_5	5	*Ca*	23	X_4	9	Y_4	9.3	12.62	13.08
S_5	5	*O-H*	23	X_5	7.4	Y_5	7.5	28.16	29.91
S_5	5	*Ca-H*	23	X_6	6.8	Y_6	7	33.98	34.58
S_5	5	*O-Co*	23	X_7	7.7	Y_7	8.1	25.24	24.30
S_5	5	*Ca-Co*	23	X_8	7.1	Y_8	7.1	31.07	33.64
S_5	5	*O-Ca*	23	X_9	8.2	Y_9	8.1	20.39	24.30
S_5	5	*O-Ca-H*	23	X_{10}	4.9	Y_{10}	5.1	52.43	52.34
S_5	5	*O-Ca-Co*	23	X_{11}	6.1	Y_{11}	6.3	40.78	41.12
S_5	10	*H*	25	X_{12}	9	Y_{12}	9	23.73	25.62
S_5	10	*Co*	25	X_{13}	9.8	Y_{13}	10	16.95	17.36
S_5	10	*O*	25	X_{14}	10.9	Y_{14}	10.7	7.63	11.57
S_5	10	*Ca*	25	X_{15}	10.1	Y_{15}	10.2	14.41	15.70
S_5	10	*O-H*	25	X_{16}	8.6	Y_{16}	8.8	27.12	27.27
S_5	10	*Ca-H*	25	X_{17}	7.7	Y_{17}	7.8	34.75	35.54
S_5	10	*O-Co*	25	X_{18}	8.9	Y_{18}	9.1	24.58	24.79
S_5	10	*Ca-Co*	25	X_{19}	8.2	Y_{19}	8.3	30.51	31.40
S_5	10	*O-Ca*	25	X_{20}	9.3	Y_{20}	9.4	21.19	22.31
S_5	10	*O-Ca-H*	25	X_{21}	5.9	Y_{21}	5.9	50.00	51.24
S_5	10	*O-Ca-Co*	25	X_{22}	7.2	Y_{22}	7.1	38.98	41.32

At the end of each experiment, water was drained off from the flume carefully to keep the scour pattern unaffected from the drawdown flushing. The scour holes and scour pattern profiles around piers were then accurately measured with the help of a depth gauge. The measuring section for the eroded profile of scour hole was chosen at about 1.0 m long along the upstream and downstream with the pier at the center (Table 2). The duration of each run was always considered as 24 h, during which the equilibrium scour depth was achieved [50]. The detail of experiments performed in the rectangular flume are shown in Figure 3.

Figure 3. Details of experiments performed in the rectangular flume.

3. Results and Discussion

3.1. Time Variation of Scour Depth at Bridge Pier Shapes

Figure 4a,b shows the temporal evolution of scour depth at the location of maximum scour depth for shapes S_2 and S_5, i.e., tests (3, 4, 15, 16) and (9, 10, 21, 22), respectively. For each of the pier shapes, the scour depth initially increased, reaching a maximum value, and then asymptotically approached a stable state. Hence, it can also be concluded that that the rate of scour depth decreases with time. From the observations, it may be noted that about 75% of the maximum scour depth was reached initially at about first four hours of the experiment, which is similar to the results obtained by Lu et al. [51].

The rate of increase of scour depth for different bed sediments (d_{50} = 0.71 mm and 0.98 mm) was the same during the initial development of scour hole; however, it was different in the long-term phase. The reason may be that as the scour hole deepens, the removal of sediment particles from the scour hole becomes more difficult. This observation is consistent with that observed by Khaple et al. [49] for different bed materials.

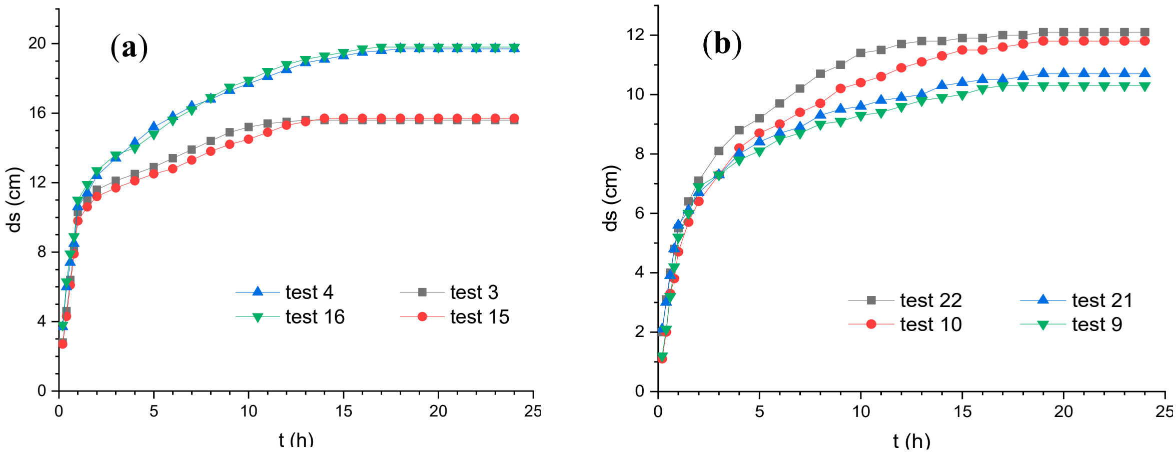

Figure 4. Time evolution of local scour depth (**a**) for shape S_2: test 3 (D_p = 5 cm, d_{50} = 0.71 mm), test 4 (D_p = 10 cm, d_{50} = 0.71 mm), test 15 (D_p = 5 cm, d_{50} = 0.98 mm), and test 16 (D_p = 10 cm, d_{50} = 0.98 mm); (**b**) for shape S_5: test 9 (D_p = 5 cm, d_{50} = 0.71 mm), test 10 (D_p = 10 cm, d_{50} = 0.71 mm), test 21 (D_p = 5 cm, d_{50} = 0.98 mm), and test 22 (D_p = 10 cm, d_{50} = 0.98 mm).

3.2. Variation of Maximum Scour Depth with Pier Size and Shape

Figure 5a,b shows the variation of final scour depth with pier size for different pier shapes. Furthermore, it demonstrates that on both median sediment sizes (d_{50} = 0.71 mm, 0.98 mm) the maximum scour depth for square pier shape (S_2) model was greater than that of other pier shape models, i.e., S_1, S_3, S_4, S_5, and S_6. Similarly, the octagonal pier shape (S_5) shows the minimum final scour depth for both median sediment sizes. It was observed that the maximum percentage reduction of scour depth for shape S_5 having pier size 5 cm was 34% and 31.8% with bed material 0.71 mm and 0.98 mm, respectively, when compared to shape S_2. Similarly, when pier size was 10 cm, the reduction of scour depth for shape S_5 was 40.1% and 38.9% when bed material was 0.71 mm and 0.98 mm, respectively. It is interesting to note that the S_5 with D_p = 10 cm had less final scour depth as compared to all other pier shapes having D_p = 5 cm, as shown in Figure 5a,b.

It is also obvious from the results that the smaller the pier size (D_p = 5 cm), the lower the scour depth, whereas higher scour depth occurred at a larger pier size (D_p = 10 cm). The reason behind this was that by increasing the pier size, the obstruction to water was increased, resulting in the enhancement of downflow and horse-shoe vortex and hence the pier scour depth.

Likewise, the comparison of final scour depth of two different bed materials, i.e., d_{50} = (0.71 mm, 0.98 mm) with pier size D_p = 5 cm and 10 cm is shown in Figure 5c,d, respectively. For the same pier size, the results revealed that the variation of sediment bed materials had less impact on final scour depth. It was observed that the maximum difference in the final scour depth of two bed materials was

3.7% and 2.5% for the case when the pier size was 5 cm and 10 cm, respectively. However, for the same bed material, the variation of pier size increased the final scour depth comprehensively. The maximum difference observed in the final scour depth of two pier sizes was 24% and 23.7% for the case when mean sediment size was 0.71 mm and 0.98 mm, respectively. The impact of bed material on final scour depth was further tested in later experiments of pier modifications.

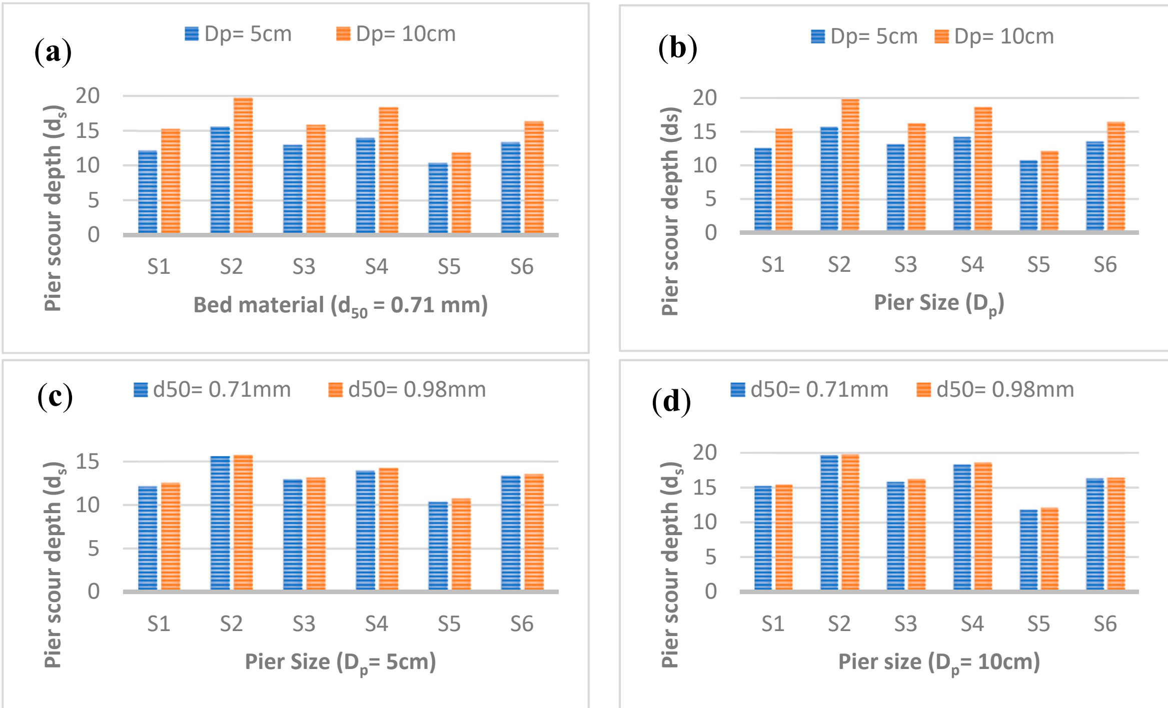

Figure 5. Comparison of scour depth for different pier shapes with different pier sizes: (**a**) d_{50} = 0.71 mm, (**b**) d_{50} = 0.98 mm; with different bed materials: (**c**) D_p = 5 cm, (**d**) D_p = 10 cm.

3.3. Scour Pattern around Bridge Pier Shapes

The formation of scour pattern around different pier shapes was quite interesting. The shapes of the piers significantly altered the scour patterns locally around the respective piers. To illustrate the scour pattern around different pier shapes, Figure 6 presents the measurements of scour depth along the transverse direction of the pier-front edge through location E_2 and also in the longitudinal streamwise direction through location E_1–E_8 of Table 2. It is noticed that on both pier sizes with varying bed materials, the length of the scoured section along the transverse and stream-wise directions was maximum for the shape S_2 and minimum for shape S_5. The decrease of scoured section length in both directions can be observed for shape S_4 and S_6, as compared to shape S_2. Likewise, shape S_1 and S_3 showed almost similar scoured length section along transverse and stream-wise directions, which were smaller than S_4 and S_6. Furthermore, it can be seen that, in front of the cylinder, the bed slopes in the sand pit for all the profiles of different pier shapes were almost the same. Both scour depths in front of and behind the cylinder increased with an increase in pier diameter. However, with the change of bed materials for each pier diameter, an almost similar pattern of scour profile was observed, for example, in Figure 5a,a′, and Figure 5c,c′. Moreover, it was monitored that the position of major deposition regions at the downstream, and the overall shape of the deformed area, occurred because of the effect of the pier shapes. Thus, it was clearly observed from the results that the occurrences of locations of maximum scour depths depended on the geometry of the shape.

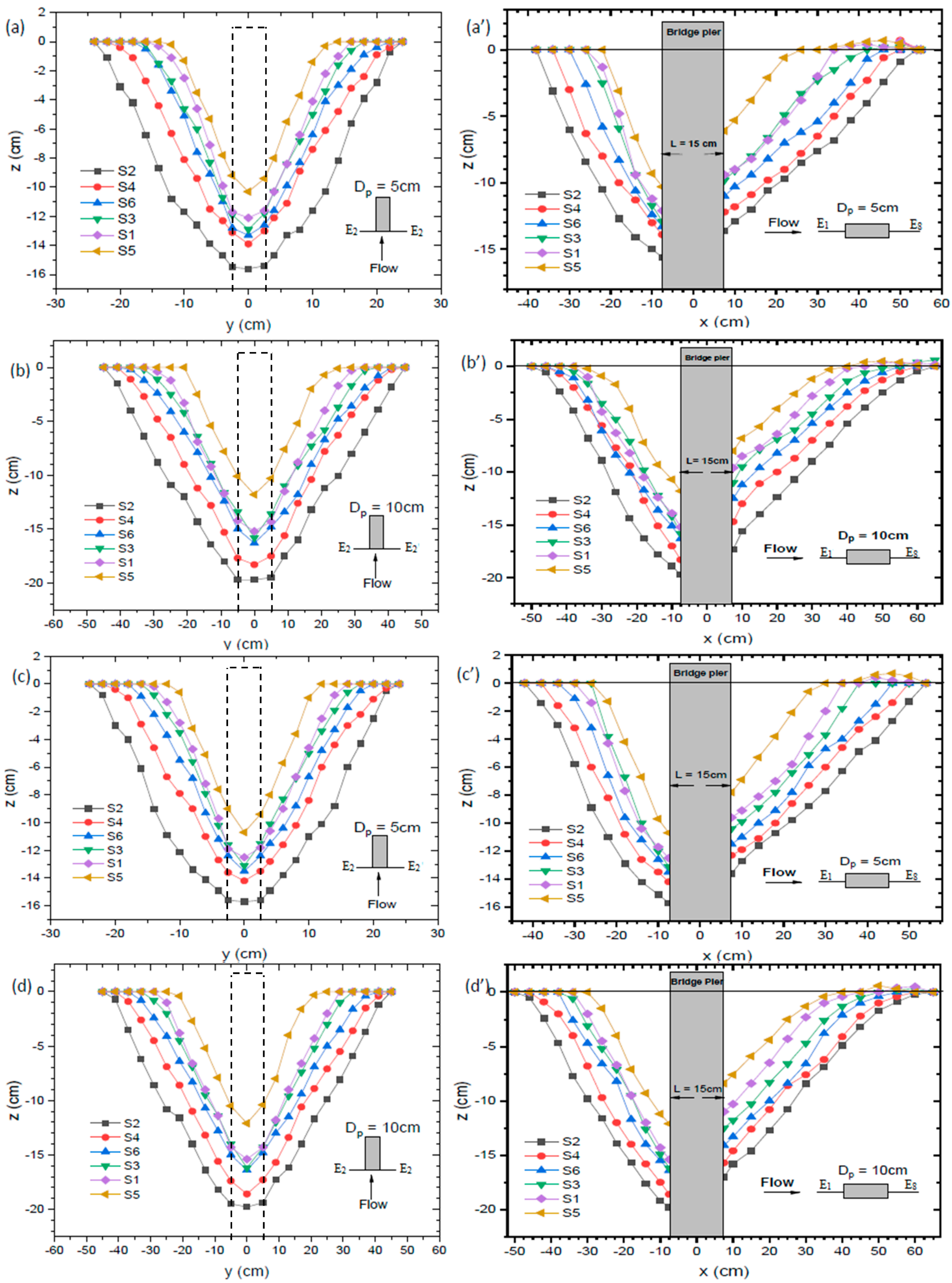

Figure 6. Scour profiles aligned with section E_2–E_2 and section E_1–E_8 for different pier shapes (**a**,**a′**,**b**,**b′**) for d_{50} = 0.71 mm; (**c**,**c′**,**d**,**d′**) for d_{50} = 0.98 mm.

3.4. Time Variation of Scour Depth at Octagonal Pier with Modifications

A detailed overview of time variation of pier modifications when applied individually, and in combination at octagonal piers, were examined under the same flow conditions. For the former case, when modifications were tested individually at an octagonal pier, the hooked collar showed much more satisfactory results as compared to all other pier modifications. Interestingly, the hooked collar has better scour reduction when compared to a collar. This is because the hooked collar blocked the downward movement of water for a greater duration, as shown in Figure 7a,b, thereby reducing the downward impact of horseshoe vortex formation. From the tests X_1-(*H*) and X_9-(*O-Ca*) (Figure 7a), and X_{12}-(*H*) and X_{20}-(*O-Ca*) (Figure 7b), it can be seen that hooked collar individually is more efficient in terms of reducing scour, as compared to combined modification of openings and cable around an octagonal pier. Moreover, the openings modification is least effective in terms of reducing scour, followed by the cable modification. Although the provision of openings provides an alternate path for the flow to move and reduces the downward flow, it was observed from the results that this reduction is very nominal to prevent the scour intrusion as compared to other modifications. Additionally, the deposition of sediments in opening holes was observed at the end of all octagonal piers with openings experiments. It can be concluded that this deposition of sediments mainly lessens the efficiency of openings when specifically applied individually. However, when this provision was applied with other modifications at the octagonal pier, it performed relatively well as compared to when it was applied individually. The main reason was that because of the provision of other modifications such as the hooked collar, collar, or cables, the downward flow was weakened and scouring initiated relatively slowly with a delay during this phase, whilst the provision of openings performed relatively well, and it also played its part to weaken the downward flow and formation of a horseshoe vortex.

In the latter case, seven combinations of different configurations were examined under the same flow conditions around the octagonal pier, i.e., *O-H*, C_a-*H*, *O*-C_o, C_a-C_o, *O*-C_a, *O*-C_a-*H*, and *O*-C_a-*Co*. The maximum scour depth for the octagonal pier with *Ca-H* was found to be less than that of the four cases, i.e., *O-H*, *O*-C_o, C_a-C_o, and *O*-C_a. The reduction in scour depth occurred because of the provision of the hooked collar in combination with the cable, causing obstruction to downward flow and resulting in a horseshoe vortex. Initially, scouring action blocked at the upstream of pier. The flow was shifted to downstream of the pier, forming a wake vortex and therein resulting in small scour pits. These pits expanded and progressed towards upstream and initiated scour depth there. Because of this delayed process, the equilibrium stage of scouring took more time. As the scouring action for the hooked collar pier started with a delay, the addition of the cable made the pier more effective as it further delayed the start of scouring, in which the equilibrium time was longer than that of the other four cases. In contrast to this, the combination of openings and cable around the pier had a greater final scour depth when compared to all other six combinations of pier configurations. The threads of cable obstructed the downward flow more effectively than the openings in the pier, but their combination was least effective in terms of reducing scouring. Hence, the combination of three modifications, i.e., provision of hooked collar, threads, and openings in the octagonal pier, resulted in the most effective configuration in reducing scour depth produced by downward flow and the formation of a horseshoe vortex.

Furthermore, the comparisons of the time variation of scour depth d_s in test series *X* with respect to that of the unprotected octagonal piers are shown in Figure 7a,b, for pier sizes D_p = 5 cm and 10 cm, respectively. In all the tests, d_s was determined at the upstream point E_2, represented in Table 2 at different time intervals. Twenty-two tests were conducted for each sediment size, i.e., overall forty-four experiments were performed for both sediment sizes. Time duration of each run was maintained as 24 h, during which the equilibrium scour depth was attained [50]. It is clear from Figure 7a,b that by applying pier modifications, a significant decrease of the equilibrium scour depth was noticed at a pier with reference to an unprotected pier. Table 3 provides the details of the experimental runs, in which different modifications were applied to the octagonal pier in two different sediment beds.

Using combined pier modifications, the rate of scour depth development further decreased and finally attained a minimum scour depth as compared to that of the unprotected pier. This phenomenon was observed in both the sediment sizes in a similar way. However, in spite of applying combined pier modifications, the time variation of scour depth was almost the same.

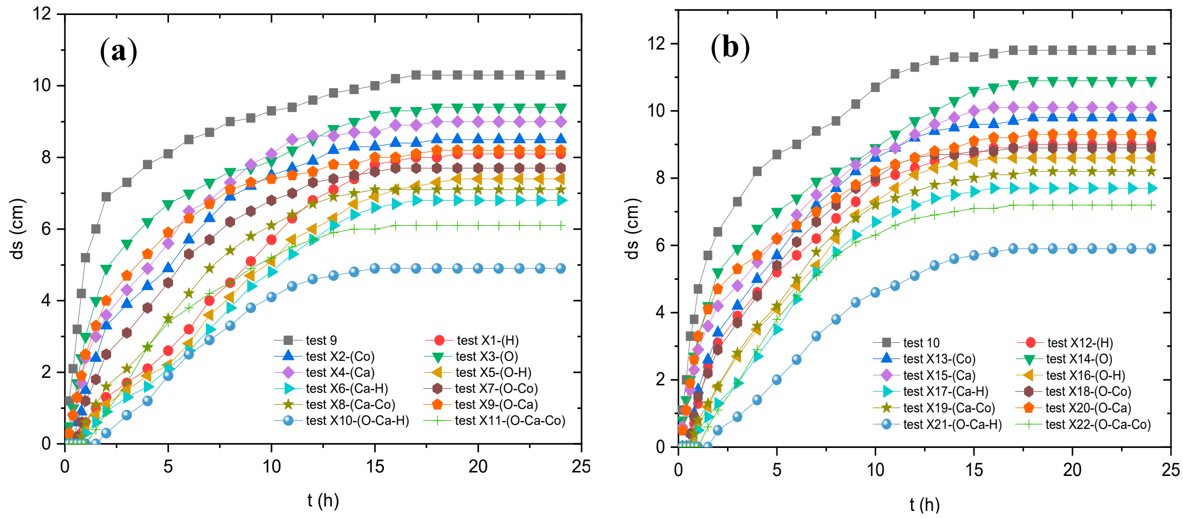

Figure 7. Comparison of the time variation of scour depths in tests of series X with pier modifications (**a**) (tests X_1–X_{11}) with respect to the corresponding test with unprotected octagonal pier (test 9), (D_p = 5 cm, d_{50} = 0.71 mm); (**b**) (tests X_{12}–X_{22}) with respect to the corresponding test with unprotected octagonal pier (test 10), (D_p = 10 cm, d_{50} = 0.71 mm).

The comparison of the time variation of scour depths in experiments of series X (d_{50} = 0.71 mm) with the corresponding tests of series Y (d_{50} = 0.98 mm) is shown in Figures 8 and 9. The temporal variation of scour depths at pier diameters D_p = 5 cm (tests X_1–X_{11}, Y_1–Y_{11}) and 10 cm (tests X_{12}–X_{22}, Y_{12}–Y_{22}) are presented in Figures 8 and 9, respectively. In these figures, the general trend of the evolution of scour depth at a pier with pier modifications is the same as that of the unprotected octagonal pier.

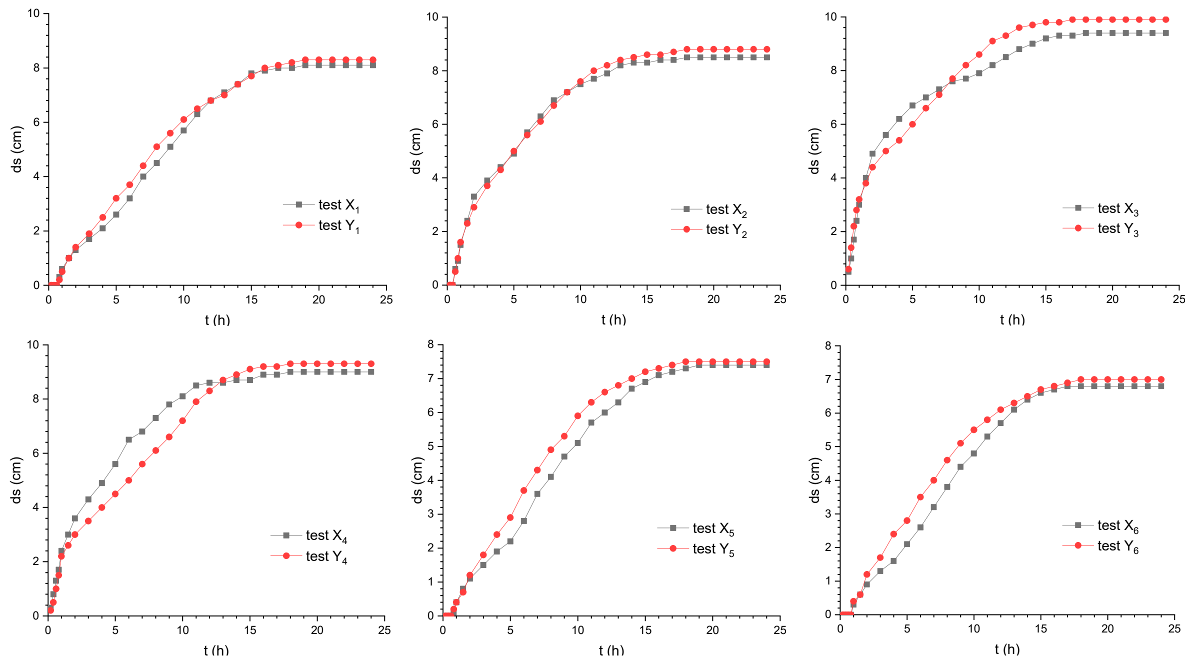

Figure 8. *Cont.*

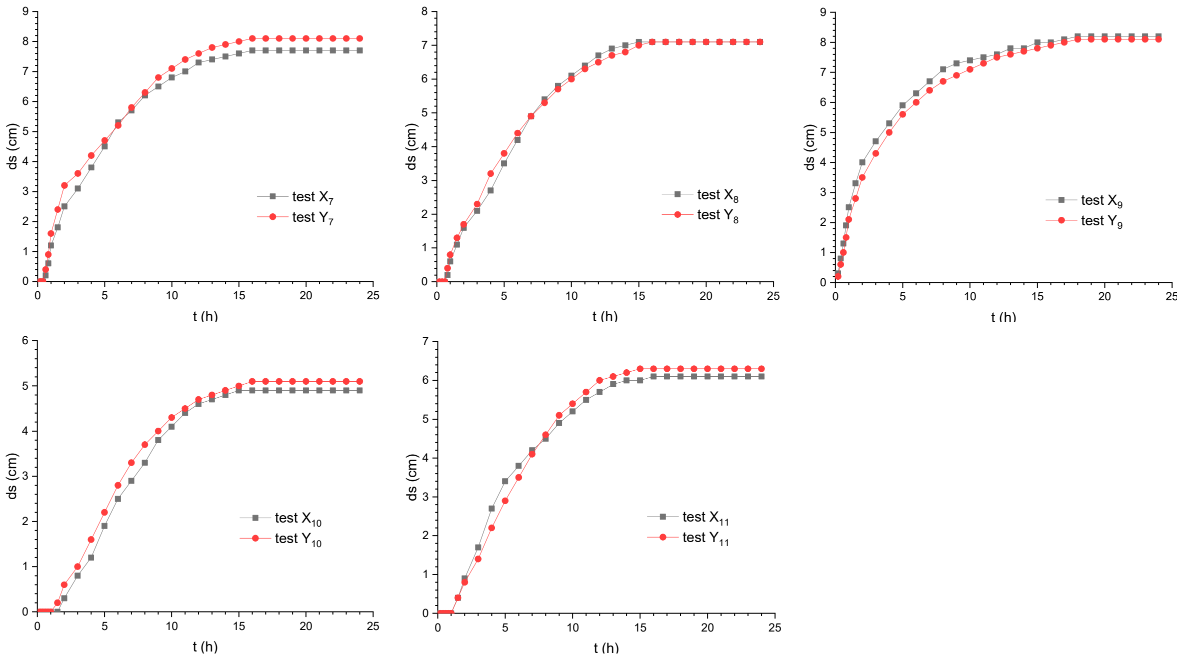

Figure 8. Comparison of the time variation of scour depths in corresponding tests of series X (d_{50} = 0.71 mm) and Y (d_{50} = 0.98 mm) with pier modifications (X_1–X_{11}, Y_1–Y_{11}; D_p = 5 cm): tests X_1 and Y_1, ... tests X_{11} and Y_{11}.

The general profile of time variation of scour depth at a pier with modifications was found to be similar in the experiments for two different sediment sizes, i.e., d_{50} = 0.71 mm and 0.98 mm, as well as for two pier sizes, namely D_p = 5 cm and 10 cm. In addition, for a given pier size, it was found that the rate of increase of scour depth was initially high for the finer sediment size d_{50} = 0.71 mm as compared to the coarser sediment size d_{50} = 0.98 mm. Interestingly, the final equilibrium scour depth was approximately the same for both the bed materials and two pier sizes, as shown in Figures 8 and 9, respectively. However, it is observed that the maximum difference in the final scour depth of two bed materials was 5.1% and 2% for the case when pier size was 5 cm and 10 cm, respectively. Furthermore, the maximum difference in final equilibrium scour depth of two pier sizes was in the range of 16.9% and 14.8% for the case when mean sediment size was 0.71 mm and 0.98 mm, respectively.

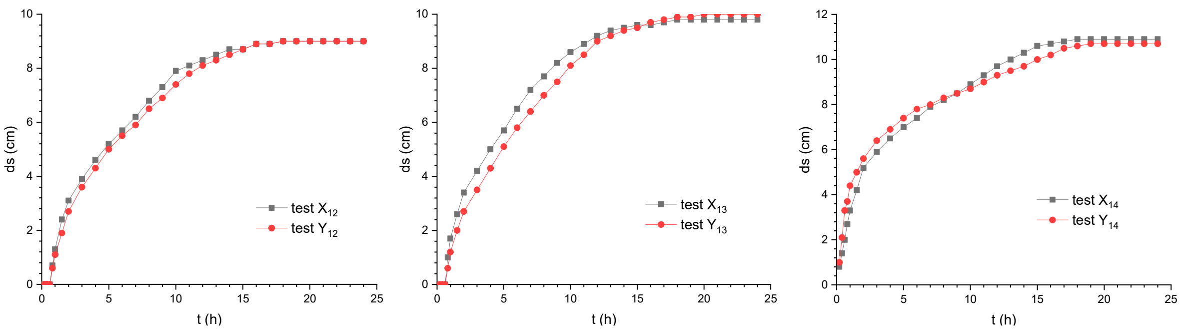

Figure 9. *Cont.*

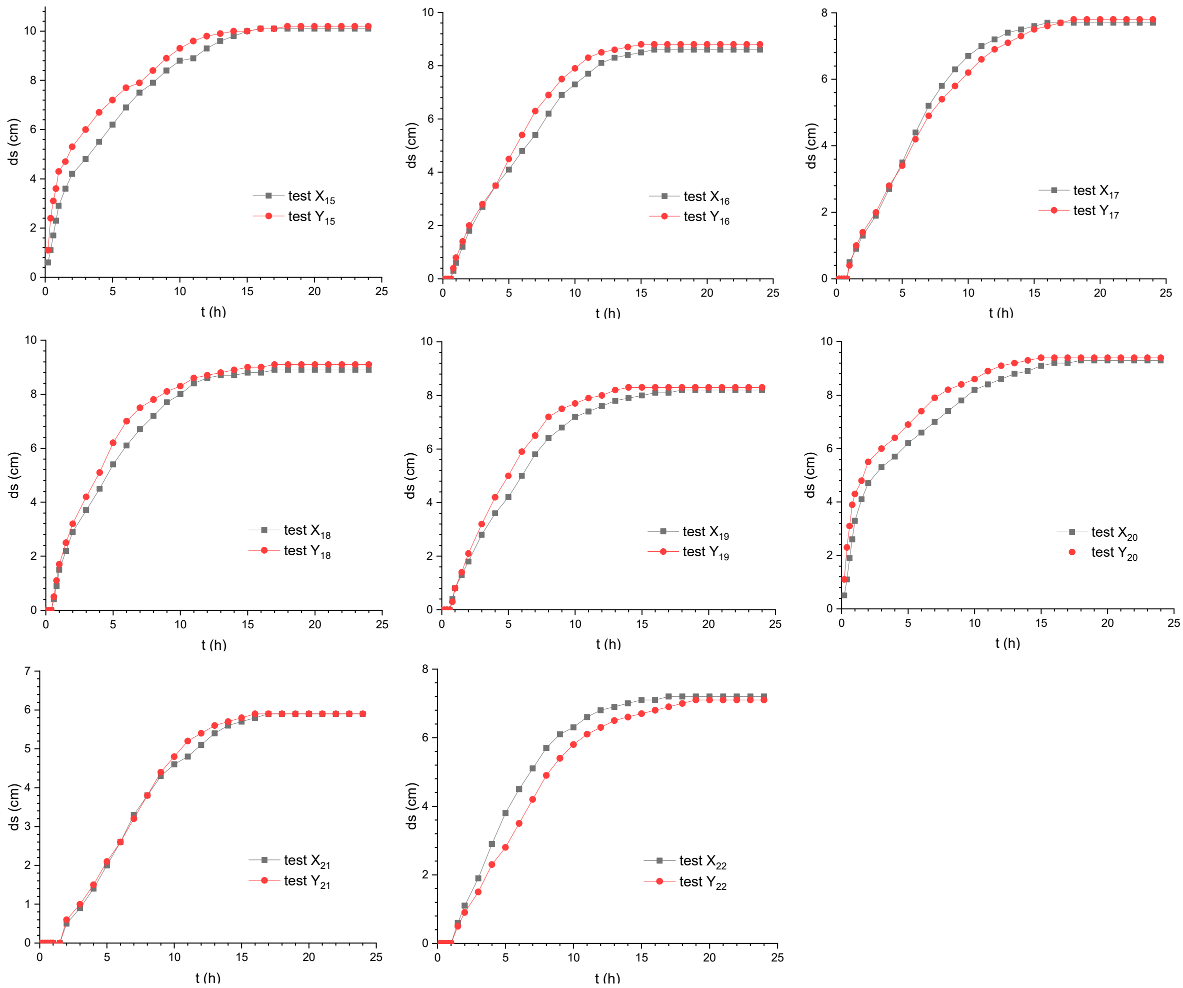

Figure 9. Comparison of the time variation of scour depths in corresponding tests of series X (d_{50} = 0.71 mm) and Y (d_{50} = 0.98 mm) with pier modifications (X_{11}–X_{22}, Y_{11}–Y_{22}; D_p = 10 cm): tests X_{11} and Y_{11}, … …. tests X_{22} and Y_{22}.

3.5. Variation of Maximum Scour Depth with Pier Sizes and Modifications

Figure 10a,b shows the variation of maximum scour depth with two pier sizes for different pier modifications and an unprotected octagonal pier. It was again observed from the results that a smaller pier size (D_p = 5 cm) has lower maximum scour depth, whereas a higher maximum scour depth occurs at a pier with a larger size (D_p = 10 cm) when they were tested against different pier modifications. Furthermore, the aforementioned figures demonstrate that on both pier sizes (D_p = 5, 10 cm) and median sediment sizes (d_{50} = 0.71 mm, 0.98 mm), the best combination of pier configuration was *O-Ca-H* around an octagonal pier. The maximum scour depth reduction for this combination was greater than that of all other pier modifications either applied around an octagonal pier individually or in combinations. It was noticed that the maximum percentage reduction (r_{ds}) was about 52.34% for octagonal piers configured with cable, openings, and the hooked collar, when compared to the unprotected octagonal pier. Comparison of maximum scour depth of pier modifications individually and in combination with different octagonal pier sizes (D_p = 5, 10 cm) and bed materials (d_{50} = 0.71, 0.98 mm) are shown in Figure 10a,b.

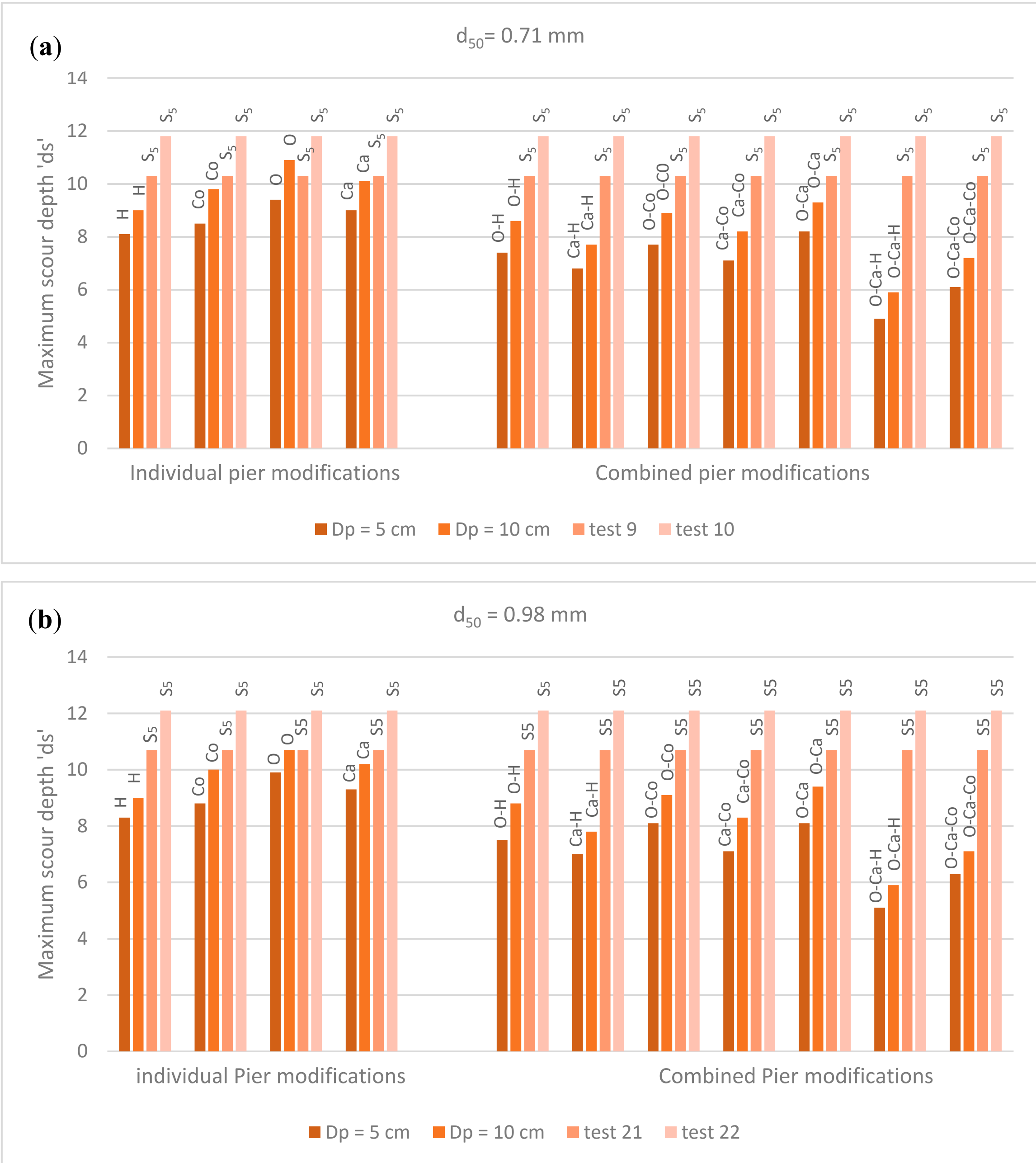

Figure 10. Comparison of maximum scour depth for protected and unprotected piers with different pier sizes: (**a**) d_{50} = 0.71 mm, (**b**) d_{50} = 0.98 mm.

3.6. Volume of Scour Hole

The volume of the scour hole V_s, which is indicative of the extent of loss of soil support to the pier foundation, was calculated for each pier modification using Simpson's 3/8th rule from the scour contour map. Table 5 shows the scour geometric parameters for all pier modifications applied around the octagonal pier individually and in combination at a pier size and median sediment size of 5 cm and 0.71 mm, respectively.

Table 5. Scour geometric parameters for D_p = 5 cm and d_{50} = 0.71 mm.

Pier Shape	Modification	D_p	d_{50} (mm)	Max. Scour Depth d_s (cm)	Percent Scour Reduction (r_{ds})	Volume of Scour Hole (m^3)	Percent Scour Reduction (r_{ds})
S_5	-	5	0.71	10.3	0	0.017	0
S_5	*H*	5	0.71	8.1	21.4	0.010	38.2
S_5	*Co*	5	0.71	8.5	17.5	0.012	31.9
S_5	*O*	5	0.71	9.4	8.7	0.014	16.7
S_5	*Ca*	5	0.71	9	12.6	0.013	23.6
S_5	*O-H*	5	0.71	7.4	28.2	0.009	48.4
S_5	*Ca-H*	5	0.71	6.8	34.0	0.007	56.4
S_5	*O-Co*	5	0.71	7.7	25.2	0.009	44.1
S_5	*Ca-Co*	5	0.71	7.1	31.1	0.008	52.5
S_5	*O-Ca*	5	0.71	8.2	20.4	0.011	36.6
S_5	*O-Ca-H*	5	0.71	4.9	52.4	0.004	77.4
S_5	*O-Ca-Co*	5	0.71	6.1	40.8	0.006	64.9

The V_s was observed to increase for the scenario when modifications around the octagonal pier were applied individually to the scenario when modifications around the octagonal pier were applied in combination. However, individually the value of V_s for the hooked collar around the octagonal pier was observed to be the minimum at 0.010 m^3. Similarly, in combinations, the value of V_s for *O-Ca-H* was found to be the minimum at 0.004 m^3. These values indicate a 38.2% and 77.4% decrease in V_s for a decrease of 21.4% and 52.4% in maximum scour depth d_s, respectively. As the streamwise and transverse extents of scour decreased with d_s, the total volume of scour hole, V_s, was also expected to decrease with d_s. The exact nature of the relationship between d_s and V_s was found by fitting an equation to the data, as shown in Figure 11. The volume of scour was seen to decrease quadratically with d_s, following the equation $V_s = 1.6{d_s}^2$, where V_s and d_s are in cubic meters and centimeters, respectively. This equation has a similar form to the equation proposed by Ebrahimi et al. [52], i.e., $V_s = 2.2{d_s}^2$, where V_s and d_s are in cubic meters and centimeters, respectively, for scour at a sharp nose pier in the presence of debris. This information can be useful in planning post-flood remedial works (e.g., Solaimani et al. [53]) where often only maximum scour depth is initially measured.

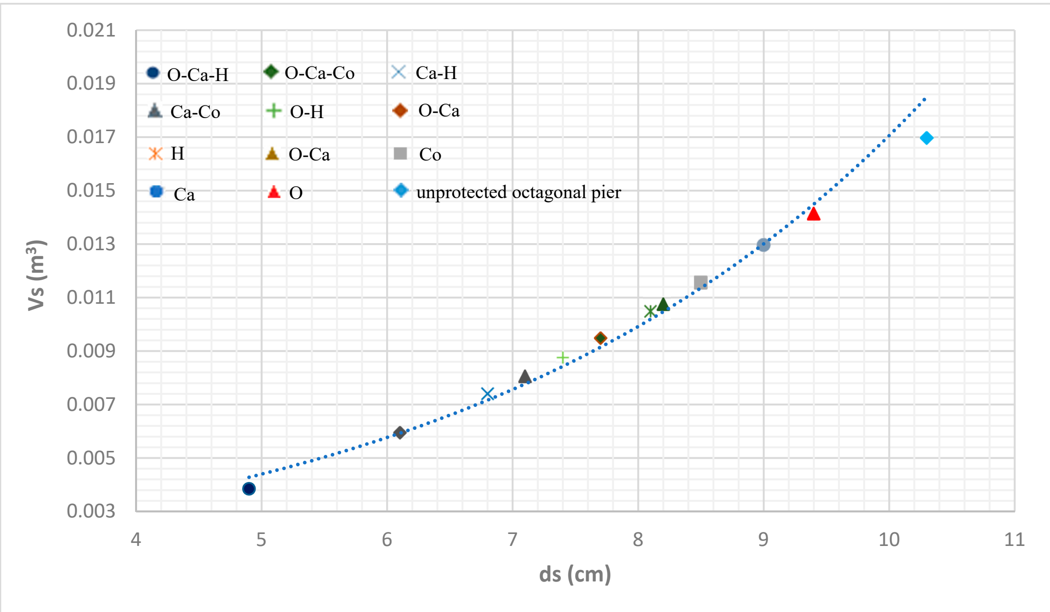

Figure 11. Volume of scour hole calculated around protected and unprotected bridge piers; dash curve is a quadratic curve ($V_s = 1.6{d_s}^2$) fitted over the data.

3.7. Scour Maps of Unprotected and Protected Octagonal Pier

Figure 12a–d respectively shows the final scour profile in the form of contour maps, measured at the end of each experiment (after 24 h). These contour plots were generated from the measurements of vertical elevations using a point gauge. Herein, the contour plots of bed form elevations (z), are discussed only for the unprotected octagonal pier and protected octagonal pier with $O\text{-}C_a\text{-}H$ modifications.

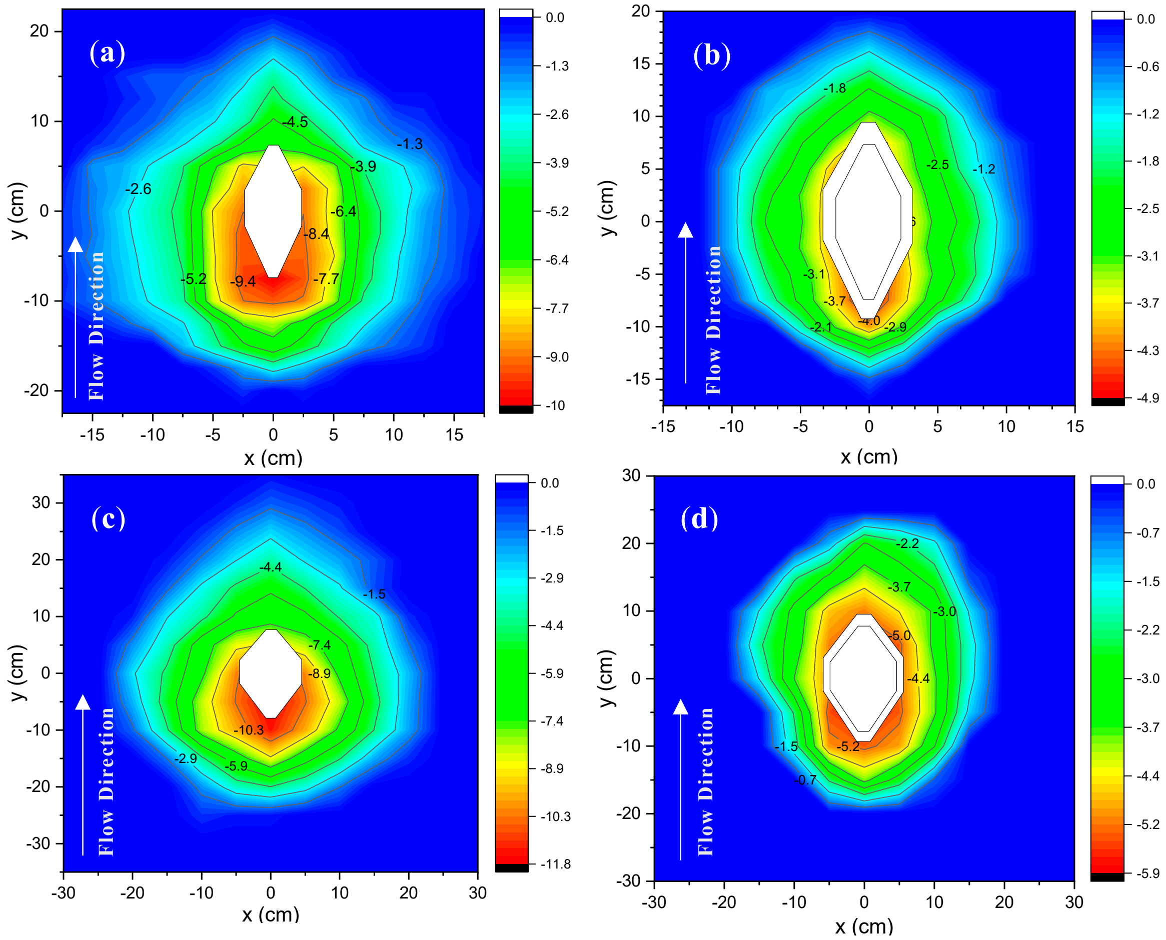

Figure 12. Equilibrium scour hole profile with different pier sizes around (**a**) and (**c**) unprotected octagonal piers with D_p = 5 and 10 cm, respectively; (**b**) and (**d**) protected octagonal pier with *O-Ca-H* modifications with D_p = 5 and 10 cm, respectively; on the same bed material (d_{50} = 0.71 mm).

It was observed from the figures that maximum scour depth was at the upstream side, mainly at the leading edges, for both the unprotected and protected octagonal pier. However, a symmetry of scour patterns was observed on both sediment bed materials with the same pier size in all cases of protected and unprotected octagonal piers. The extent of the scour pattern was greatly reduced at the longitudinal and transverse direction for the case when a provision of $O\text{-}C_a\text{-}H$ was applied around the octagonal pier, as compared to the unprotected octagonal pier.

4. Conclusions

This experimental study aimed at assessing the most efficient pier shape in terms of reducing scour and also the capability of various pier modifications to minimize the erosive power of flow acting on the riverbed around that efficient pier shape. The work has extended previous published studies by considering six pier shapes (namely circular, rectangular, rhombus, sharp nose, octagonal and elliptical) and four pier modifications (namely collar, openings, cables, and hooked collar), under clear water conditions. The scour measurement was conducted whilst the flow was running. The scour development time history, equilibrium scour depth, and volume of scour hole were studied, together with the three-dimensional scour-hole profiles.

The main conclusions from this work are as follows:

1. Under the same conditions, the maximum scour depth around six different pier shapes was monitored on different pier sizes (D_p = 5 cm, 10 cm) and bed materials (d_{50} = 0.71 mm, 0.98 mm). It is interesting to note that octagonal pier shape is the most effective in reducing the scour depth, followed by the circular pier shape. In comparison with the rectangular pier, which is the least effective in reducing scour depth, the percentage of scour reduction for circular, rhombus, sharp nose, octagonal, and elliptical piers were 17.7, 22.4, 10.9, 33.8, and 15.1, respectively, for pier size D_p = 5 cm and median sediment size d_{50} = 0.71 mm. Furthermore, a similar sequence of scour reduction was observed for D_p = 10 cm.
2. The shape of a pier is an important parameter in the scouring process. We recommended an octagonal pier as the most suitable form of pier geometry for applying pier modification countermeasures separately and in combination.
3. When applying pier modifications separately around an unprotected octagonal pier, the hooked collar is the most effective in protecting the pier against local scour, followed by the collar. In comparison with the unprotected octagonal pier without any modification, the percentage of scour reduction for the hooked collar (*H*), collar (*Co*), openings (*O*), and cables (*Ca*) were 21.4, 17.5, 8.7, and 12.6, respectively, for pier size D_p = 5 cm and median sediment size d_{50} = 0.71 mm.
4. The combination of the hooked collar, cables, and openings (*O-Ca-H*) was more effective in reducing scour when compared to the other six cases. In comparison with the unprotected octagonal pier without any modification, the percentage of scour reduction for *O-H*, *Ca-H*, *O-Co*, *Ca-Co*, *O-Ca*, *O-Ca-H*, and *O-Ca-Co* were 28.2, 34, 25.2, 31.1, 20.4, 52.4, and 40.8, respectively, for pier size D_p = 5 cm and median sediment size d_{50} = 0.71 mm.
5. In all pier shapes and pier modification experiments on different pier sizes (D_p = 5 cm, 10 cm), the smaller size pier was more effective than the larger pier size, indicating that the larger the pier size, the larger the scour depth. Similarly, it was also confirmed from the results that behavior of scour on different pier shapes was almost the same in all experiments.
6. The longitudinal and transverse extents of scour increased with scour depth. The volume of scour hole increased quadratically with maximum scour depth after 24 h. This trend was similar to what was found in previous research for scenarios with debris. The proposed equation can be useful for calculating the volume of material required for filling scour holes in post-flood remedial field works in which only maximum scour depth is measured.

Supplementary Materials: The following are available online at http://www.mdpi.com/2073-4441/11/9/1761/s1, Table S1: Geometric parameters of pier shapes.

Author Contributions: Piers and modifications design, laboratory experiments, writing: R.F. Data verification, review: A.R.G.

Funding: This research received no external funding.

Acknowledgments: The authors are thankful to the three anonymous reviewers of this work.

Conflicts of Interest: The authors declare no conflict of interest.

References

1. Lee, C.H.; Xu, C.; Huang, Z. A three-phase flow simulation of local scour caused by a submerged wall jet with a water-air interface. *Adv. Water Resour.* **2019**, *129*, 373–384. [CrossRef]
2. Melville, B.W.; Coleman, S.E. *Bridge Scour*; Water Resources Publications: Highlands Ranch, CO, USA, 2000.
3. Zokaei, M.; Zarrati, A.R.; Salamatian, S.A.; Karimaee Tabarestani, M. Study on scouring around bridge piers protected by collar using low density sediment. *Int. J. Civ. Eng.* **2013**, *11*, 199–205.
4. Zarrati, R.A.; Nazariha, M.; Mashahir, M.B. Reduction of Local Scour in the Vicinity of Bridge Pier Groups Using Collars and Riprap. *J. Hydraul. Eng.* **2006**, *132*, 154–162. [CrossRef]

5. Singh, K.U.; Ahmad, Z.; Kumar, A. Turbulence characteristics of flow over the degraded cohesive bed of clay–silt–sand mixture. *ISH J. Hydraul. Eng.* **2017**, *23*, 308–318. [CrossRef]
6. Pandey, M.; Ahmad, Z.; Sharma, P.K. Flow-characteristics around circular pier model. In Proceedings of the HYDRO'15 International Conference, IIT ROORKEE, Roorkee, India, 17–19 December 2015.
7. Melville, B.W. Pier and Abutment Scour: Integrated Approach. *J. Hydraul. Eng.* **1997**, *123*, 125–136. [CrossRef]
8. Melville, B.W. Live-bed Scour at Bridge Piers. *J. Hydraul. Eng.* **1984**, *110*, 1234–1247. [CrossRef]
9. Dargahi, B. Controlling Mechanism of Local Scouring. *J. Hydraul. Eng.* **1990**, *116*, 1197–1214. [CrossRef]
10. Yanmaz, M.A.; Üstün, I. Generalized reliability model for local scour around bridge piers of various shapes. *Turk. J. Eng. Environ. Sci.* **2001**, *25*, 687–698.
11. Zarrati, A.R.; Gholami, H.; Mashahir, M. Application of collar to control scouring around rectangular bridge piers. *J. Hydraul. Res.* **2004**, *42*, 97–103. [CrossRef]
12. Fael, C.; Lança, R.; Cardoso, A. Effect of pier shape and pier alignment on the equilibrium scour depth at single piers. *Int. J. Sediment Res.* **2016**, *31*, 244–250. [CrossRef]
13. Vijayasree, B.A.; Eldho, T.I.; Mazumder, B.S.; Ahmad, N. Influence of bridge pier shape on flow field and scour geometry. *Int. J. River Basin Manag.* **2017**, *17*, 109–129. [CrossRef]
14. Kirkil, G.; Constantinescu, S.G.; Ettema, R. Coherent structures in the flow field around a circular cylinder with scour hole. *J. Hydraul. Eng.* **2008**, *134*, 572–587. [CrossRef]
15. Escauriaza, C.; Sotiropoulos, F. Initial stages of erosion and bed form development in a turbulent flow around a cylindrical pier. *J. Geophys. Res. Earth Surf.* **2011**, *116*. [CrossRef]
16. Link, O.; González, C.; Maldonado, M.; Escauriaza, C. Coherent structure dynamics and sediment particle motion around a cylindrical pier in developing scour holes. *Acta Geophys.* **2012**, *60*, 1689–1719. [CrossRef]
17. Apsilidis, N.; Diplas, P.; Dancey, C.L.; Bouratsis, P. Time-resolved flow dynamics and Reynolds number effects at a wall–cylinder junction. *J. Fluid Mech.* **2015**, *776*, 475–511. [CrossRef]
18. Bouratsis, P.; Diplas, P.; Dancey, C.L.; Apsilidis, N. High-resolution 3-D monitoring of evolving sediment beds. *Water Resour. Res.* **2013**, *49*, 977–992. [CrossRef]
19. Chen, Q.; Qi, M.; Zhong, Q.; Li, D. Experimental study on the multimodal dynamics of the turbulent horseshoe vortex system around a circular cylinder. *Phys. Fluids* **2017**, *29*, 015106. [CrossRef]
20. Ettema, R.; Constantinescu, G.; Melville, B.W. Flow-Field Complexity and Design Estimation of Pier-Scour Depth: Sixty Years since Laursen and Toch. *J. Hydraul. Eng.* **2017**, *143*, 03117006. [CrossRef]
21. Manes, C.; Brocchini, M. Local scour around structures and the phenomenology of turbulence. *J. Fluid Mech.* **2015**, *779*, 309–324. [CrossRef]
22. Fael, C.; Lança, R.; Cardoso, A. Pier shape and alignment effects on local scour. In *SHF Conference: Small Scale Morphological Evolution of Costal, Estuarine and River Systems*; Societe Hydrotecnique de France: Paris, France, 2014.
23. Al-Shukur, A.-H.K.; Obeid, Z.H. Experimental study of bridge pier shape to minimize local scour. *Int. J. Civil Eng. Technol.* **2016**, *7*, 162–171.
24. Murtaza, G.; Hashmi, H.N.; Naeem, U.A.; Khan, D.; Ahmad, N. Effect of Bridge Pier Shape on Scour Depth at Uniform Single Bridge Pier. *Mehran Univ. Res. J. Eng. Technol.* **2018**, *37*, 539–544. [CrossRef]
25. Kumar, V.; Raju, K.G.R.; Vittal, N. Reduction of local scour around bridge piers using slots and collars. *J. Hydraul. Eng.* **1999**, *125*, 1302–1305. [CrossRef]
26. Moncada-M, A.T.; Aguirre-Pe, J.; Bolivar, J.C.; Flores, E.J. Scour protection of circular bridge piers with collars and slots. *J. Hydraul. Res.* **2009**, *47*, 119–126. [CrossRef]
27. EL-Ghorab, E.A. Reduction of scour around bridge piers using a modified method for vortex reduction. *Alex. Eng. J.* **2013**, *52*, 467–478. [CrossRef]
28. Wang, C.; Yu, X.; Liang, F. A review of bridge scour: Mechanism, estimation, monitoring and countermeasures. *Nat. Hazards* **2017**, *87*, 1881–1906. [CrossRef]
29. Garg, V.; Setia, B.; Verma, D. Reduction of scour around a bridge pier by multiple collar plates. *ISH J. Hydraul. Eng.* **2005**, *11*, 66–80. [CrossRef]
30. Izadinia, E.; Heidarpour, M. Simultaneous use of cable and collar to prevent local scouring around bridge pier. *Int. J. Sediment Res.* **2012**, *27*, 394–401. [CrossRef]
31. Kumcu, S.Y.; Kokpinar, M.A.; Gogus, M. Scour protection around vertical-wall bridge abutments with collars. *KSCE J. Civ. Eng.* **2014**, *18*, 1884–1895. [CrossRef]

32. Khosravinia, P.; Malekpour, A.; Hosseinzadehdalir, A.; Farsadizadeh, D. Effect of trapezoidal collars as a scour countermeasure around wing-wall abutments. *Water Sci. Eng.* **2018**, *11*, 53–60. [CrossRef]
33. Salamatian, S.A.; Zarrati, A.R. Reliability study on uncertainty parameters and flood duration on scouring around unprotected and protected bridge piers. *ISH J. Hydraul. Eng.* **2019**, 1–9. [CrossRef]
34. Alabi, P.D. Time Development of Local Scour at A Bridge Pier Fitted with A Collar. Ph.D. Thesis, University of Saskatchewan, Saskatchewan, SK, Canada, 2006.
35. Dey, S.; Sumer, B.M.; Fredsøe, J. Control of scour at vertical circular piles under waves and current. *J. Hydraul. Eng.* **2006**, *132*, 270–279. [CrossRef]
36. Saadati, S.; Heydari, M.M.; Saneie, M. Experimental investigation of ridged collar effect on scour process on the periphery of circular pier in clear water condition. *Fresen. Env. Bull* **2016**, *25*, 4525–4536.
37. Chen, S.C.; Tfwala, S.; Wu, T.Y.; Chan, H.C.; Chou, H.T. Ahooked-collar for bridge piers protection: Flow fields and scour. *Water* **2018**, *10*, 1251. [CrossRef]
38. Tafarojnoruz, A.; Gaudio, R.; Dey, S. Flow-altering countermeasures against scour at bridge piers: A review. *J. Hydraul. Res.* **2010**, *48*, 441–452. [CrossRef]
39. Tafarojnoruz, A.; Gaudio, R.; Calomino, F. Evaluation of flow-altering countermeasures against bridge pier scour. *J. Hydraul. Eng.* **2012**, *138*, 297–305. [CrossRef]
40. Farooq, R.; Ghumman, A.R.; Hashmi, H.N. Influence of Pier Modification Techniques for Reducing Scour around Bridge Piers. *World Acad. Sci. Eng. Technol. Int. J. Civ. Environ. Struct. Constr. Archit. Eng.* **2017**, *11*, 462–468.
41. Gaudio, R.; Tafarojnoruz, A.; Calomino, F. Combined flow-altering countermeasures against bridge pier scour. *J. Hydraul. Res.* **2012**, *50*, 35–43. [CrossRef]
42. Zarrati, A.R.; Chamani, M.R.; Shafaie, A.; Latifi, M. Scour countermeasures for cylindrical piers using riprap and combination of collar and riprap. *Int. J. Sediment Res.* **2010**, *25*, 313–322. [CrossRef]
43. Chiew, Y.; Melville, B. Local scour around bridge piers. *J. Hydraul. Res.* **1987**, *25*, 15–26. [CrossRef]
44. Ettema, R. Scour at Bridge Piers. Ph.D. Thesis, University of Auckland, Auckland, New Zealand, 1980.
45. Lauchlan, C.S.; Melville, B.W. Riprap protection at bridge piers. *J. Hydraul. Eng.* **2001**, *127*, 412–418. [CrossRef]
46. Khaple, S. Effects of an Upstream Bridge Pier on Scour at Downstream Bridge Piers and Scour Countermeasure. Ph.D. Thesis, Indian Institute of Technology, Kharagpur, India, 2018.
47. Ballio, F.; Teruzzi, A.; Radice, A. Constriction effects in clear-water scour at abutments. *J. Hydraul. Eng.* **2009**, *135*, 140–145. [CrossRef]
48. Lança, R.; Fael, C.; Maia, R.; Pêgo, J.P.; Cardoso, A.H. Clear-Water Scour at Pile Groups. *J. Hydraul. Eng.* **2013**, *139*, 1089–1098. [CrossRef]
49. Khaple, S.; Hanmaiahgari, P.R.; Gaudio, R.; Dey, S. Splitter plate as a flow-altering pier scour countermeasure. *Acta Geophys.* **2017**, *65*, 957–975. [CrossRef]
50. Melville, B.W.; Chiew, Y.-M. Time Scale for Local Scour at Bridge Piers. *J. Hydraul. Eng.* **1999**, *125*, 59–65. [CrossRef]
51. Lu, J.-Y.; Shi, Z.Z.; Hong, J.H.; Lee, J.J.; Raikar, R.V. Temporal Variation of Scour Depth at Nonuniform Cylindrical Piers. *J. Hydraul. Eng.* **2011**, *137*, 45–56. [CrossRef]
52. Ebrahimi, M.; Kripakaran, P.; Prodanović, D.M.; Kahraman, R.; Riella, M.; Tabor, G.; Arthur, S.; Djordjević, S. Experimental Study on Scour at a Sharp-Nose Bridge Pier with Debris Blockage. *J. Hydraul. Eng.* **2018**, *144*, 04018071. [CrossRef]
53. Solaimani, N.; Amini, A.; Banejad, H.; Taherei Ghazvinei, P. The effect of pile spacing and arrangement on bed formation and scour hole dimensions in pile groups. *Int. J. River Basin Manag.* **2017**, *15*, 219–225. [CrossRef]